Journal of Energy

VOLUME 61 | 2012

journal homepage: http://journalofenergy.com/

Branimir Ćućić, Ph.D
Končar - Distribution and Special Transformers Inc.
branimir.cucic@koncar-dst.hr

MAGNETIC FIELD COMPUTATION OF A LOADED TRANSFORMER

SUMMARY

A simple numerical method based on integral approach was described to compute the stray magnetic field in the surrounding region of a loaded distribution transformer. The model for magnetic field computation was made of transformer windings and low voltage conductors. Windings were modeled by rectangular and round blocks with uniform amper-turn distribution throughout the winding cross section. Low voltage conductors were modeled as series of straight current-carrying wire segments. The computed and measured results of magnetic induction are in good agreement.

Key words: loaded distribution transformer, stray magnetic field, magnetic induction

1. INTRODUCTION

The sensitivity of population regarding the electromagnetic emissions has significantly increased over the last fifteen years, mainly due to intensive use of mobile phones. In this paper extremely low frequency magnetic field of the transformer is to be determined. The term "extremely low frequencies" (ELF) is commonly used to describe any frequency below 300 Hz, in this case 50 Hz.

The magnetic induction reference level at 50 Hz recommended by ICNIRP is 100 μT for the public exposure, and 500 μT for the occupational exposure [1]. ICNIRP guidelines are based on short-term, immediate health effects. Most of the European countries follow these guidelines. However, some countries have decided to take a more precautionary approach by lowering the limits for exposure (Switzerland - 1 μT [2], Italy - 3 μT [3], Slovenia – 10 μT [4], Croatia – 40 μT [5], etc.).

Another issue is electromagnetic compatibility. ELF magnetic field can cause interference with electronic devices even if the field value is below reference level.

Distribution transformer as a part of power system generates 50 Hz magnetic field. The stray magnetic field in the surrounding region of a transformer is usually determined in short circuit test [3], [6] where low voltage windings are shorted and rated currents flow through all windings. However, such determined magnetic field can be significantly different from the field generated by loaded transformer. The reason for that are low voltage conductors, usually cables and busbars, through which transformer is loaded. In many practical cases they are the main source of the magnetic field. In this paper one such case was analyzed. A simple numerical method based on integral approach was described to compute quasistatic magnetic field of a loaded distribution transformer. The field was determined in the area above a 1000 kVA distribution transformer placed in a substation.

2. GEOMETRY AND MAIN TECHNICAL DATA

Analyzed configuration is shown in Figure 1. A voltage is applied to the primary side (high voltage side) of the distribution transformer. Load is connected to the secondary. The magnetic field was computed in two planes in the office room above the transformer (z=2.48 m and z=3.48 m). The origin of the coordinate system (z=0) was set at the top of the transformer tank.

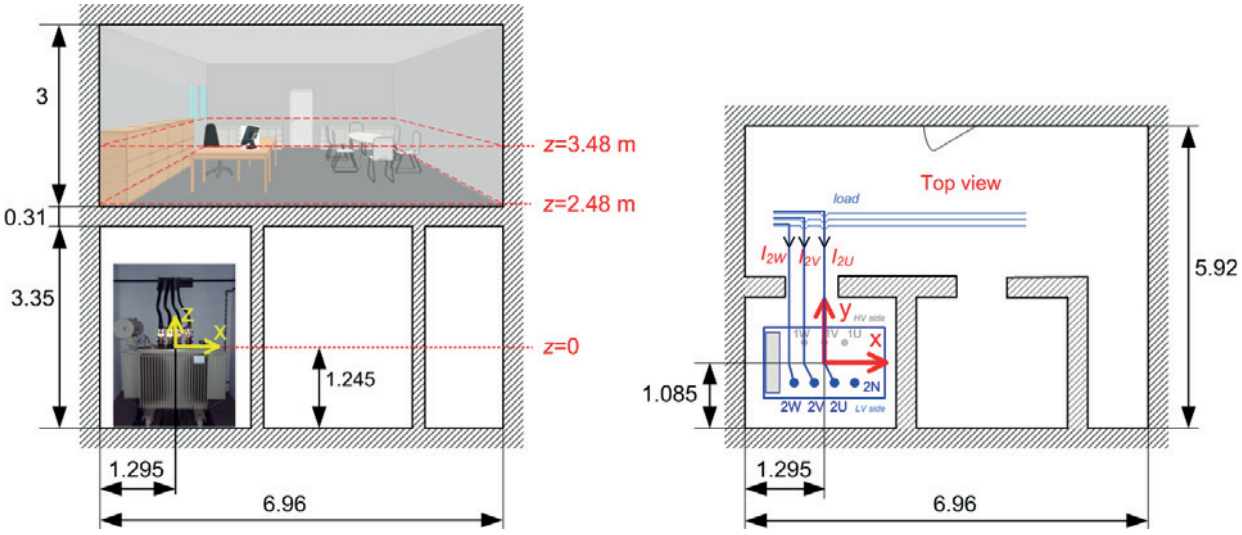

Figure 1 - Geometry of the problem. Dimensions are in meters

Transformer technical data are given in Table I.

Table I. Transformer technical data

Type	Three-phase oil immersed distribution transformer
Rated power	1000 kVA
Rated high voltage	20(10) kV
Rated low voltage	420 V
Vector group	Dyn5
Impedance voltage	6 %
Rated current through HV terminals	28.9 (57.7) A
Rated current through LV terminals	1375 A
Rated current in HV windings	16.7 A
Rated current in LV windings	1375 A
Rated number of turns in HV winding	1568
Rated number of turns in LV winding	19

3. MODEL OF THE LOADED TRANSFORMER IN THE SUBSTATION

3.1. Model of the loaded transformer

The sources of the magnetic field are all current-carrying elements. According to Figure 2, these sources are low voltage (LV) and high voltage (HV) windings, leads, cables and busbars. In configuration shown in Figure 1, where magnetic field is computed in the planes 2.48 m and 3.48 m far from the transformer tank cover, main source of the magnetic field are LV cables. Magnetic field in these planes is not significantly influenced by the transformer core, tank, clamping system or any other part of transformer substation, the reason why all these parts were ignored. Furthermore, the current in HV side is 10000/420 ≈ 24 times lower than current in LV side. Because of that, all HV conductors, except windings, were ignored.

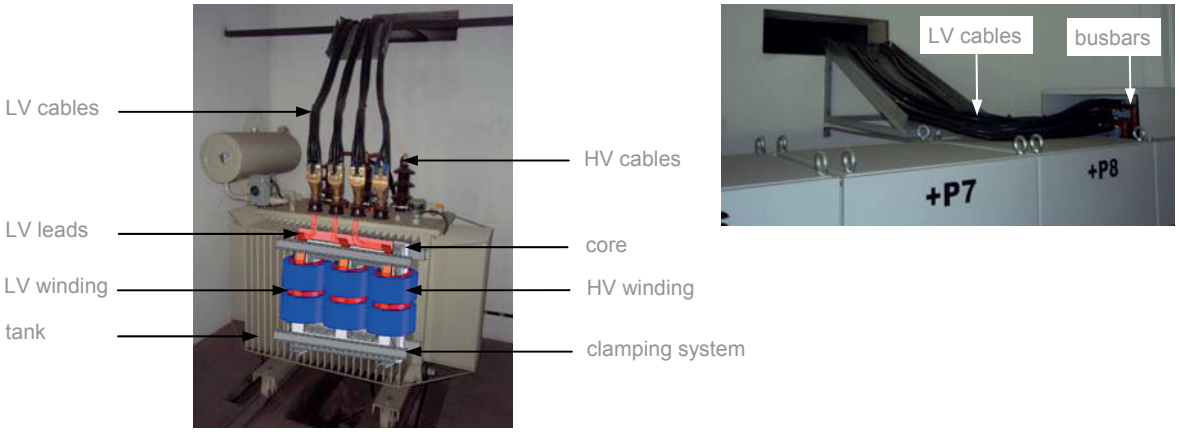

Figure 2 - Main parts of loaded transformer in the substation

The loaded transformer in the transformer substation was modeled by using transformer windings and all LV conductors (leads, cables and busbars) [7]. The model is shown in Figure 3.

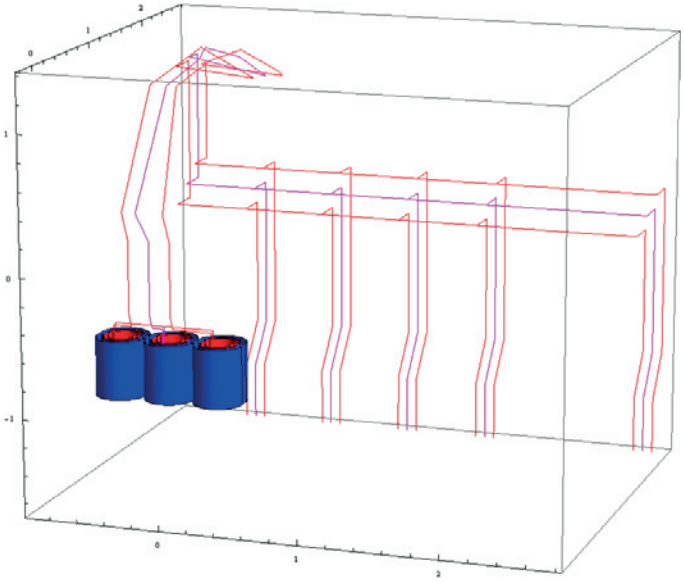

Figure 3 - Model of loaded transformer for the magnetic field computation

3.2. Model of the winding

Windings were modeled by rectangular and round blocks with uniform amper-turn distribution throughout the winding cross section as illustrated in Figure 4, where:

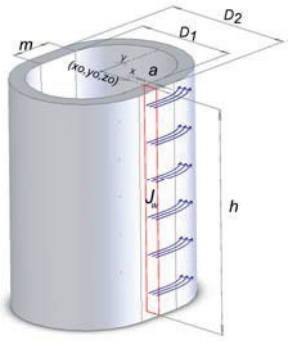

Figure 4 - Model of oval winding

D_1 – inner diameter of the winding
D_2 – outer diameter of the winding
a – winding width
m – length of straight part of oval winding
(xo,yo,zo) – coordinates of the center of the upper part of the winding
h – winding height
J_W – winding current density (A/mm^2)
$I_{ph} \cdot W$ – amperturns

Input data for all windings are given in Table II.

Table II. Input data for all windings

	LV phases			HV phases		
	a	b	c	A	B	C
D_1 (m)	0.179			0.260		
D_2 (m)	0.244			0.345		
m (m)	0.079			0.079		
xo (m)	0.354	0	-0.354	0.354	0	-0.354
yo (m)	0			0		
zo (m)	-0.407			-0.415		
h (m)	0.424			0.408		
$\dot{I}_{ph} \cdot W$ (Amperturns)	26118	$26118 \cdot e^{j \cdot (-120°)}$	$26118 \cdot e^{j \cdot 120°}$	–26118	$-26118 \cdot e^{j \cdot (-120°)}$	$-26118 \cdot e^{j \cdot 120°}$

3.3. Model of LV conductors

LV conductors were modeled as series of straight current-carrying thin wire segments. According to Figure 5, every straight wire segment carrying current I is defined by start coordinates (x_1,y_1,z_1) and end coordinates (x_2,y_2,z_2).

Figure 5 - A straight wire segment carrying current I

Input data for all straight current-carrying wire segments are given in Table III.
The current through each straight wire segment is $k \cdot 1375$ in "a" phase, $k \cdot 1375\ e^{j \cdot (-120°)}$ in "b" phase, and $k \cdot 1375\ e^{j \cdot 120°}$ in "c" phase.

Table III. Input data for straight current-carrying wire segments

Phase	x_1 (m)	y_1 (m)	z_1 (m)	x_2 (m)	y_2 (m)	z_2 (m)	k	x_1 (m)	y_1 (m)	z_1 (m)	x_2 (m)	y_2 (m)	z_2 (m)	k
a	0.35	-0.16	-0.41	0.35	-0.16	-0.30	-1	0.37	2.48	0.28	0.37	2.73	0.28	-0.35
	0.35	-0.16	-0.30	0.08	-0.16	-0.30	-1	0.37	2.73	0.28	0.37	2.73	-0.95	-0.35
	0.08	-0.16	-0.30	0.08	-0.20	-0.20	-1	0.37	2.73	-0.95	0.37	2.48	-1.24	-0.35
	0.08	-0.20	-0.20	0.08	-0.20	0.31	-1	0.37	2.48	-1.24	0.37	2.48	-1.64	-0.35
	0.08	-0.20	0.31	-0.05	0.00	0.45	-1	0.37	2.48	0.28	0.97	2.48	0.28	-0.5
	-0.05	0.00	0.45	-0.11	0.43	1.26	-1	0.97	2.48	0.28	0.97	2.73	0.28	-0.15
	-0.11	0.43	1.26	-0.11	1.10	1.33	-1	0.97	2.73	0.28	0.97	2.73	-0.95	-0.15
	-0.11	1.10	1.33	0.00	1.41	1.36	-1	0.97	2.73	-0.95	0.97	2.48	-1.24	-0.15
	0.00	1.41	1.36	0.00	2.21	1.07	-1	0.97	2.48	-1.24	0.97	2.48	-1.64	-0.15
	0.00	2.21	1.07	-0.13	2.63	0.96	-1	0.97	2.48	0.28	1.57	2.48	0.28	-0.35
	-0.13	2.63	0.96	-0.77	2.63	1.01	-1	1.57	2.48	0.28	1.57	2.73	0.28	-0.15
	-0.77	2.63	1.01	-0.77	2.73	1.01	-1	1.57	2.73	0.28	1.57	2.73	-0.95	-0.15
	-0.77	2.73	1.01	-0.77	2.73	0.28	-1	1.57	2.73	-0.95	1.57	2.48	-1.24	-0.15
	-0.77	2.73	0.28	-0.77	2.48	0.28	-1	1.57	2.48	-1.24	1.57	2.48	-1.64	-0.15
	-0.77	2.48	0.28	-0.23	2.48	0.28	-1	1.57	2.48	0.28	2.77	2.48	0.28	-0.2
	-0.23	2.48	0.28	-0.23	2.73	0.28	-0.15	2.77	2.48	0.28	2.77	2.73	0.28	-0.2
	-0.23	2.73	0.28	-0.23	2.73	-0.95	-0.15	2.77	2.73	0.28	2.77	2.73	-0.95	-0.2
	-0.23	2.73	-0.95	-0.23	2.48	-1.24	-0.15	2.77	2.73	-0.95	2.77	2.48	-1.24	-0.2
	-0.23	2.48	-1.24	-0.23	2.48	-1.64	-0.15	2.77	2.48	-1.24	2.77	2.48	-1.64	-0.2
	-0.23	2.48	0.28	0.37	2.48	0.28	-0.85	0.35	-0.13	-0.41	0.35	-0.13	-0.29	1
								0.35	-0.13	-0.29	0.00	-0.13	-0.29	1

Phase	x_1 (m)	y_1 (m)	z_1 (m)	x_2 (m)	y_2 (m)	z_2 (m)	k	x_1 (m)	y_1 (m)	z_1 (m)	x_2 (m)	y_2 (m)	z_2 (m)	k
b	0.00	-0.16	-0.41	0.00	-0.16	-0.30	-1	0.30	2.48	0.12	0.30	2.73	0.12	-0.35
	0.00	-0.16	-0.30	-0.08	-0.16	-0.30	-1	0.30	2.73	0.12	0.30	2.73	-0.95	-0.35
	-0.08	-0.16	-0.30	-0.08	-0.20	-0.20	-1	0.30	2.73	-0.95	0.30	2.48	-1.24	-0.35
	-0.08	-0.20	-0.20	-0.08	-0.20	0.31	-1	0.30	2.48	-1.24	0.30	2.48	-1.64	-0.35
	-0.08	-0.20	0.31	-0.25	0.00	0.45	-1	0.30	2.48	0.12	0.90	2.48	0.12	-0.5
	-0.25	0.00	0.45	-0.18	0.43	1.26	-1	0.90	2.48	0.12	0.90	2.73	0.12	-0.15
	-0.18	0.43	1.26	-0.20	1.10	1.33	-1	0.90	2.73	0.12	0.90	2.73	-0.95	-0.15
	-0.20	1.10	1.33	-0.27	1.41	1.36	-1	0.90	2.73	-0.95	0.90	2.48	-1.24	-0.15
	-0.27	1.41	1.36	-0.13	1.71	1.26	-1	0.90	2.48	-1.24	0.90	2.48	-1.64	-0.15
	-0.13	1.71	1.26	-0.24	2.58	0.96	-1	0.90	2.48	0.12	1.50	2.48	0.12	-0.35
	-0.24	2.58	0.96	-0.84	2.58	1.07	-1	1.50	2.48	0.12	1.50	2.73	0.12	-0.15
	-0.84	2.58	1.07	-0.84	2.73	1.07	-1	1.50	2.73	0.12	1.50	2.73	-0.95	-0.15
	-0.84	2.73	1.07	-0.84	2.73	0.12	-1	1.50	2.73	-0.95	1.50	2.48	-1.24	-0.15
	-0.84	2.73	0.12	-0.84	2.48	0.12	-1	1.50	2.48	-1.24	1.50	2.48	-1.64	-0.15
	-0.84	2.48	0.12	-0.30	2.48	0.12	-1	1.50	2.48	0.12	2.70	2.48	0.12	-0.2
	-0.30	2.48	0.12	-0.30	2.73	0.12	-0.15	2.70	2.48	0.12	2.70	2.73	0.12	-0.2
	-0.30	2.73	0.12	-0.30	2.73	-0.95	-0.15	2.70	2.73	0.12	2.70	2.73	-0.95	-0.2
	-0.30	2.73	-0.95	-0.30	2.48	-1.24	-0.15	2.70	2.73	-0.95	2.70	2.48	-1.24	-0.2
	-0.30	2.48	-1.24	-0.30	2.48	-1.64	-0.15	2.70	2.48	-1.24	2.70	2.48	-1.64	-0.2
	-0.30	2.48	0.12	0.30	2.48	0.12	-0.85	0.00	-0.13	-0.41	0.00	-0.13	-0.29	1

Phase	x_1 (m)	y_1 (m)	z_1 (m)	x_2 (m)	y_2 (m)	z_2 (m)	k	x_1 (m)	y_1 (m)	z_1 (m)	x_2 (m)	y_2 (m)	z_2 (m)	k
c	-0.35	-0.16	-0.41	-0.35	-0.16	-0.30	-1	0.23	2.48	-0.04	0.23	2.73	-0.04	-0.35
	-0.35	-0.16	-0.30	-0.23	-0.16	-0.30	-1	0.23	2.73	-0.04	0.23	2.73	-0.95	-0.35
	-0.23	-0.16	-0.30	-0.23	-0.20	-0.20	-1	0.23	2.73	-0.95	0.23	2.48	-1.24	-0.35
	-0.23	-0.20	-0.20	-0.23	-0.20	0.31	-1	0.23	2.48	-1.24	0.23	2.48	-1.64	-0.35
	-0.23	-0.20	0.31	-0.35	0.00	0.45	-1	0.23	2.48	-0.04	0.83	2.48	-0.04	-0.5
	-0.35	0.00	0.45	-0.30	0.43	1.26	-1	0.83	2.48	-0.04	0.83	2.73	-0.04	-0.15
	-0.30	0.43	1.26	-0.30	1.10	1.33	-1	0.83	2.73	-0.04	0.83	2.73	-0.95	-0.15
	-0.30	1.10	1.33	-0.30	1.41	1.36	-1	0.83	2.73	-0.95	0.83	2.48	-1.24	-0.15
	-0.30	1.41	1.36	-0.30	2.47	0.96	-1	0.83	2.48	-1.24	0.83	2.48	-1.64	-0.15
	-0.30	2.47	0.96	-0.35	2.48	0.96	-1	0.83	2.48	-0.04	1.43	2.48	-0.04	-0.35
	-0.35	2.48	0.96	-0.91	2.48	1.01	-1	1.43	2.48	-0.04	1.43	2.73	-0.04	-0.15
	-0.91	2.48	1.01	-0.91	2.73	1.01	-1	1.43	2.73	-0.04	1.43	2.73	-0.95	-0.15
	-0.91	2.73	1.01	-0.91	2.73	-0.04	-1	1.43	2.73	-0.95	1.43	2.48	-1.24	-0.15
	-0.91	2.73	-0.04	-0.91	2.48	-0.04	-1	1.43	2.48	-1.24	1.43	2.48	-1.64	-0.15
	-0.91	2.48	-0.04	-0.37	2.48	-0.04	-1	1.43	2.48	-0.04	2.63	2.48	-0.04	-0.2
	-0.37	2.48	-0.04	-0.37	2.73	-0.04	-0.15	2.63	2.48	-0.04	2.63	2.73	-0.04	-0.2
	-0.37	2.73	-0.04	-0.37	2.73	-0.95	-0.15	2.63	2.73	-0.04	2.63	2.73	-0.95	-0.2
	-0.37	2.73	-0.95	-0.37	2.48	-1.24	-0.15	2.63	2.73	-0.95	2.63	2.48	-1.24	-0.2
	-0.37	2.48	-1.24	-0.37	2.48	-1.64	-0.15	2.63	2.48	-1.24	2.63	2.48	-1.64	-0.2
	-0.37	2.48	-0.04	0.23	2.48	-0.04	-0.85	-0.35	-0.13	-0.41	-0.35	-0.13	-0.29	1
								-0.35	-0.13	-0.29	0.00	-0.13	-0.29	1

4. MAGNETIC FIELD COMPUTATION

The analysis of the magnetic field was made in phasor domain, meaning that every sinusoidal function of time was represented as a phasor which encodes the magnitude and phase angle of the sinusoid. In this paper phasor is denoted by a point above the letter (eg. current $\dot{I}$), vector by a bold letter (eg. position vector $\boldsymbol{R}$), and phasor-vector by a point above a bold letter (eg. magnetic induction $\dot{\boldsymbol{B}}$).

Magnetic induction is computed at a point (x,y,z). First, the magnetic induction of each winding ($\dot{\boldsymbol{B}}_w$) is computed, then the magnetic induction of every straight current-carrying wire segment ($\dot{\boldsymbol{B}}_L$). After that, the contribution of all windings and all straight wire segments are summarized ($\dot{\boldsymbol{B}}$). Finally, the magnetic induction is transformed into time-domain (B). All magnitudes are assumed to be RMS.

4.1. Magnetic field of a winding

Magnetic induction of a winding $\dot{\boldsymbol{B}}_w$ is computed as follows [8]:

$$\dot{\boldsymbol{B}}_w(\boldsymbol{r}) = \frac{\mu_0}{4\pi} \int_{V_o} \dot{J}_w \cdot \boldsymbol{a}_w(\boldsymbol{r}') \, x \, \frac{\boldsymbol{R}}{R^3} dV' \tag{1}$$

where: $\dot{J}_w$ – winding current density (A/mm^2)

$\boldsymbol{a}_w(\boldsymbol{r}')$ – unit vector to specify the direction of the current through the winding

dV' – differential element of volume V_o of the winding

$\boldsymbol{R}$ – position vector

R – distance between the observation (x,y,z) and the integration point (x',y',z')

μ_0 – permeability of air ($\mu_0 = 1{,}256 \cdot 10^{-6}$ H/m)

$$\dot{J}_w = \frac{\dot{I}_{ph} \cdot W}{a \cdot h} \tag{2}$$

$$\boldsymbol{R} = \boldsymbol{r} - \boldsymbol{r}' = (x - x')\boldsymbol{a}_x + (y - y')\boldsymbol{a}_y + (z - z')\boldsymbol{a}_z \tag{3}$$

$$R = \sqrt{(x - x')^2 + (y - y')^2 + (z - z')^2} \tag{4}$$

4.2. Magnetic field of a straight wire segment

Biot-Savart's law was applied to the magnetic field computation of a straight wire segment carrying current $\dot{I}$ [8]. According to Figure 6, $d\dot{\boldsymbol{B}}_L$ is magnetic induction contribution at point (x,y,z) from the current element $\dot{I}\,d\ell$:

$$d\dot{\boldsymbol{B}}_L = \frac{\mu_0 \dot{I}\, d\ell \times \boldsymbol{R}}{4\pi R^3} \tag{5}$$

$\boldsymbol{R}$ is position vector pointing from the current element $\dot{I}\,d\ell$ towards the point (x,y,z) at which $d\dot{\boldsymbol{B}}_L$ is computed.

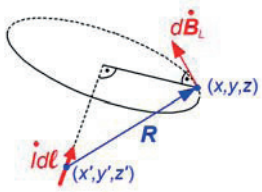

Figure 6 - Magnetic field contribution of a current element

As depicted in Figure 7, the straight current-carrying wire segment is defined by start (x_1,y_1,z_1) and end coordinates (x_2,y_2,z_2). To compute the magnetic induction $\dot{\boldsymbol{B}}_L$ of such segment, the origin of new coordinate system S" is set up at the midpoint (x_0,y_0,z_0) of the segment in a way that the current $\dot{I}$ flows in the direction of +x" axis. Magnetic induction is first computed in the local coordinate system S" and then transformed into main coordinate system S.

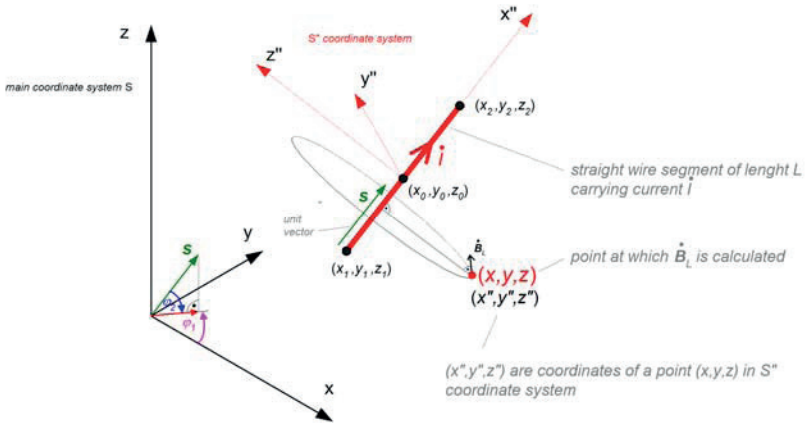

Figure 7 - Magnetic field of a straight current-carrying wire segment

The components of the phasor-vector $\dot{\boldsymbol{B}}_L$ are computed at the point (x,y,z) as follows:

$$x_0 = \frac{x_1 + x_2}{2}; \quad y_0 = \frac{y_1 + y_2}{2}; \quad z_0 = \frac{z_1 + z_2}{2}; \tag{6}$$

$$L = \sqrt{(x_2 - x_1)^2 + (y_2 - y_1)^2 + (z_2 - z_1)^2} \tag{7}$$

$$s_x = \frac{x_2 - x_1}{L}; \quad s_y = \frac{y_2 - y_1}{L}; \quad s_z = \frac{z_2 - z_1}{L} \tag{8}$$

$$k_1 = \cos\varphi_1 = \frac{s_x}{\sqrt{s_x^2 + s_y^2}}; \quad k_2 = \sin\varphi_1 = \frac{s_y}{\sqrt{s_x^2 + s_y^2}} \tag{9}$$

$$k_3 = \cos\varphi_2 = \frac{\sqrt{s_x^2 + s_y^2}}{\sqrt{s_x^2 + s_y^2 + s_z^2}}; \quad k_4 = \sin\varphi_2 = \frac{-s_z}{\sqrt{s_x^2 + s_y^2 + s_z^2}} \tag{10}$$

$$x'' = (x - x_0)\cdot k_1 \cdot k_3 + (y - y_0)\cdot k_2 \cdot k_3 - (z - z_0)\cdot k_4 \tag{11}$$

$$y'' = -(x - x_0)\cdot k_2 + (y - y_0)\cdot k_1 \tag{12}$$

$$z'' = (x - x_0)\cdot k_1 \cdot k_4 + (y - y_0)\cdot k_2 \cdot k_4 + (z - z_0)\cdot k_3 \tag{13}$$

$$d_1 = x'' + \frac{L}{2}; \quad d_2 = x'' - \frac{L}{2} \tag{14}$$

$$d_3 = \sqrt{y''^2 + z''^2} \tag{15}$$

$$R_1 = \sqrt{d_1^2 + d_3^2}; \quad R_2 = \sqrt{d_2^2 + d_3^2}; \tag{16}$$

$$\dot{B}_{Lx} = \frac{\mu_0 \dot{I}}{4\pi d_3^2}\cdot\left(\frac{d_1}{R_1} - \frac{d_2}{R_2}\right)\cdot(y''\cdot k_1 \cdot k_4 + z''\cdot k_2) \tag{17}$$

$$\dot{B}_{Ly} = \frac{\mu_0 \dot{I}}{4\pi d_3^2}\cdot\left(\frac{d_1}{R_1} - \frac{d_2}{R_2}\right)\cdot(y''\cdot k_2 \cdot k_4 - z''\cdot k_1) \tag{18}$$

$$\dot{B}_{Lz} = \frac{\mu_0 \dot{I}}{4\pi d_3^2}\cdot\left(\frac{d_1}{R_1} - \frac{d_2}{R_2}\right)\cdot y''\cdot k_3 \tag{19}$$

Equations (9) – (19) are not valid when a current-carrying segment is parallel to z-axis.

In this special case, components of $\dot{\boldsymbol{B}}_L$ are calculated as follows:

$$d_1 = z - z_o + \frac{L}{2}; \quad d_2 = z - z_o - \frac{L}{2} \tag{20}$$

$$d_3 = \sqrt{(x - x_o)^2 + (y - y_o)^2} \tag{21}$$

$$R_1 = \sqrt{d_1^2 + d_3^2}; \quad R_2 = \sqrt{d_2^2 + d_3^2}; \tag{22}$$

$$\dot{B}_{Lx} = -\frac{\mu_0 \dot{I}}{4\pi d_3^2}\cdot\left(\frac{d_1}{R_1} - \frac{d_2}{R_2}\right)\cdot(y - y_o)\cdot s_z \tag{23}$$

$$\dot{B}_{Ly} = \frac{\mu_0 \dot{I}}{4\pi d_3^2}\cdot\left(\frac{d_1}{R_1} - \frac{d_2}{R_2}\right)\cdot(x - x_o)\cdot s_z \tag{24}$$

$$\dot{B}_{Lz} = 0 \tag{25}$$

Finally, the magnetic induction of a straight wire segment in phasor domain is given by:

$$\dot{\boldsymbol{B}}_L = \dot{B}_{Lx}\,\boldsymbol{a}_x + \dot{B}_{Ly}\,\boldsymbol{a}_y + \dot{B}_{Lz}\,\boldsymbol{a}_z \tag{26}$$

4.3. Total magnetic field

Summarizing the contribution of all windings and all straight current-carrying wire segments, total magnetic induction is:

$$\dot{\boldsymbol{B}} = \sum_{i=1}^{N_w} \dot{\boldsymbol{B}}_{wi} + \sum_{j=1}^{N_L} \dot{\boldsymbol{B}}_{Lj} = \dot{B}_x\,\boldsymbol{a}_x + \dot{B}_y\,\boldsymbol{a}_y + \dot{B}_z\,\boldsymbol{a}_z \tag{27}$$

where:

N_w – number of windings (N_w = 6 for above case of a three phase transformer)
N_L – number of straight current-carrying wire segments (N_L = 122 for above case)

RMS value of magnetic induction in time domain is given by [9]:

$$B = \sqrt{\left|\dot{B}_x\right|^2 + \left|\dot{B}_y\right|^2 + \left|\dot{B}_z\right|^2} = \sqrt{B_x^{\,2} + B_y^{\,2} + B_z^{\,2}} \tag{28}$$

where B_x, B_y and B_z are magnitudes of the components $\dot{B}_x$, $\dot{B}_y$ and $\dot{B}_z$ of the phasor-vector $\dot{\boldsymbol{B}}$.

5. COMPARISON BETWEEN COMPUTATIONS AND MEASUREMENTS

Magnetic field was computed and measured in the rectangular region ABCD (1.365 m x 2.4 m) in two planes (z=2.48 m and z=3.48 m) above the transformer and LV conductors (Figure 8).

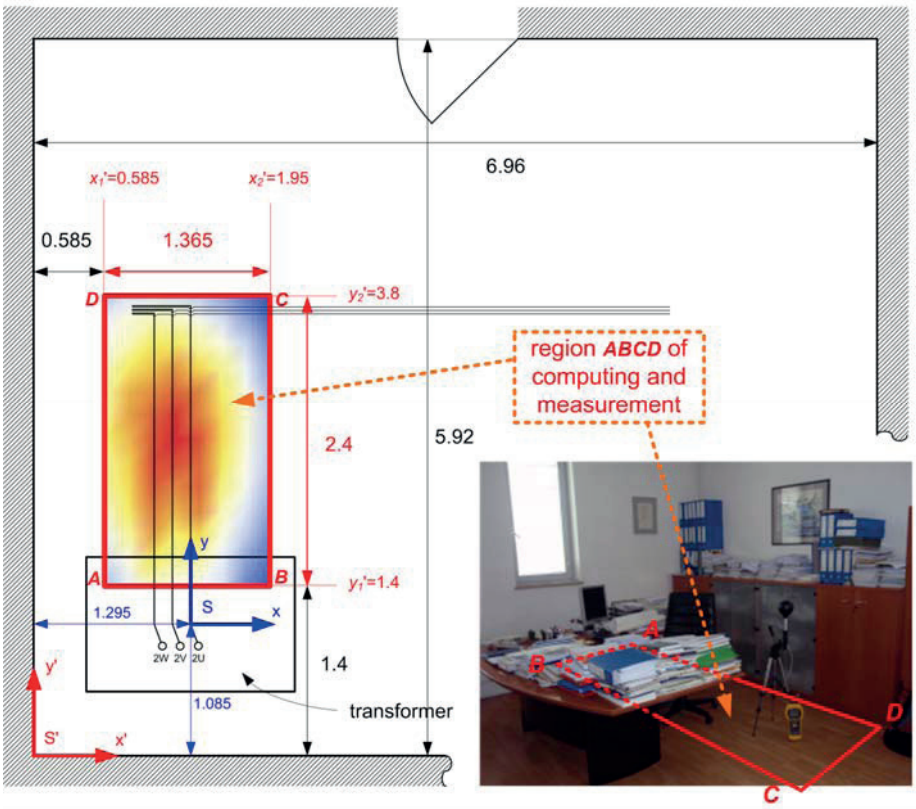

Figure 8 - Region of computing and measurement

Magnetic induction was measured by using CA 42 fieldmeter. The field was measured at average load of 46 % (638 A ± 15%). Maximum load asymmetry was 10 % and it was ignored in the model. Measured values of magnetic induction were normalized to values corresponding to nominal current by multiplying them by 1375/638. Normalized measured results of magnetic induction were compared with computed results at rated load. The results are shown in Figures 9-12.

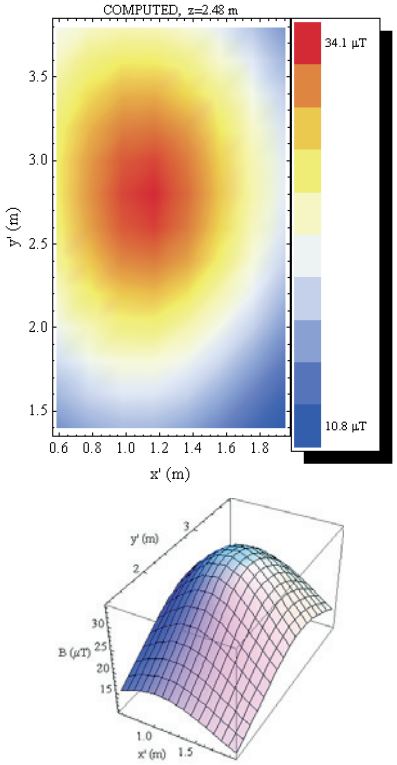

Figure 9 - Computed results for plane z=2.48 m

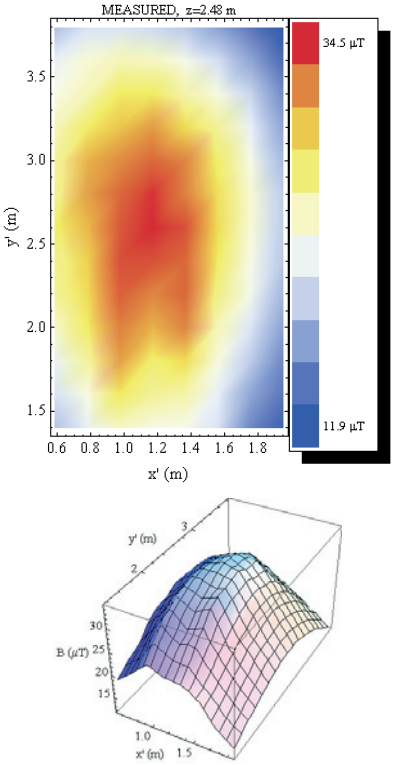

Figure 10 - Measured results for plane z=2.48 m

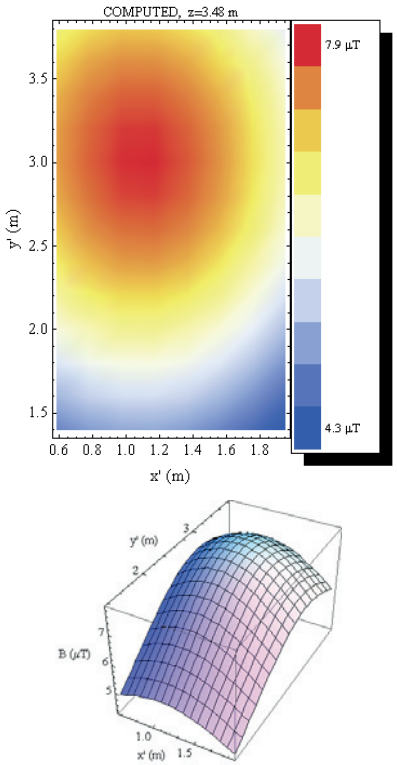

Figure 11 - Computed results for plane z=3.48 m

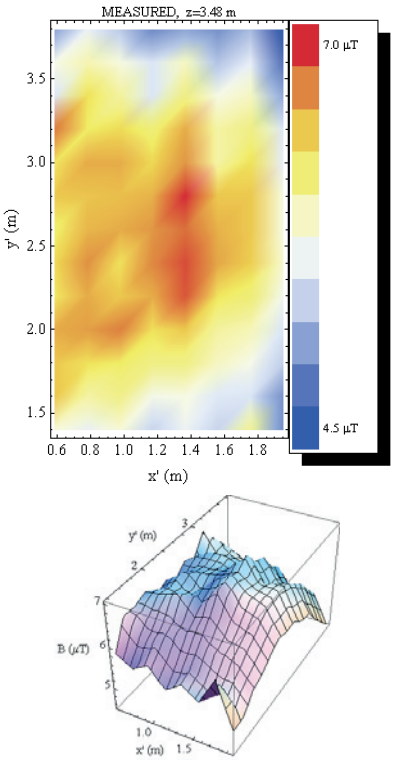

Figure 12 - Measured results for plane z=3.48 m

The results show the highest value of magnetic induction at rated load to be 34.5 μT. That was measured in the plane 6.5 cm above the floor level (z=2.48 m). In the plane 106.5 cm above the floor level (z=3.48 m) the highest computed value is 7.9 μT (measured 7 μT). Since the field was computed in the area of occupational exposure, all values are far below the limits recommended by ICNIRP (500 μT) [1] or required by Croatian ordinance (100 μT) [5]. However, those field values can cause interference with electronic devices. For example, if the computer is in such area, then image movement (jitter) on the CRT monitor screen may be noticed. This problem can be solved by replacing CRT monitor with LCD.

The comparison shows that there is a good agreement between computations and measurements. Deviation between them for the highest values of magnetic induction is 1 %, in plane z=2.48 m, and 13 % in plane z=3.48 m.

Depending on the place where the magnetic field is computed, the model can be simplified by omitting the windings. This can be done if the LV conductors are the most dominating source of the magnetic field, like in this particular case. Computations on a simplified model gave almost the same results as for the model with windings. The difference for the highest value of magnetic induction is not more than 1 %.

6. CONCLUSION

The proposed method of evaluating low frequency stray magnetic field in the surrounding region of a loaded distribution transformer appears to be very effective and practical. The method was validated by comparison with measurements. The results of the computations and measurements are in good agreement. Field values are far below the limits recommended by ICNIRP or required by Croatian ordinance. The advantage of proposed method is that no commercial magnetic field software is needed.

7. REFERENCES

[1] "ICNIRP Guidelines for Limiting Exposure to Time-Varying Electric, Magnetic and Electromagnetic Fields (up to 300 GHz)", ICNIRP, 1998.

[2] "Ordinance relating to Protection from Non-Ionising Radiation (ONIR)", The Swiss Federal Council, 1999.

[3] M. Breschi, A. Christofolini, "Experimental and numerical analysis of stray field from transformers", IEEE Transactions on Magnetics, Vol. 43, No. 11, November 2007.

[4] "Uredba o elektromagnetnem sevanju v naravnem in življenskem okolju", Uradni list št. 70, 1996.

[5] "Pravilnik o zaštiti od elektromagnetskih polja", Ministarstvo zdrastva RH, 2003.

[6] B. Ćućić, "Magnetic field in the vicinity of distribution transformers", International Colloquium Transformer Research and Asset Management, Cavtat, Croatia, November 12 – 14, 2009.

[7] I. Kapetanović, V. Madžarević, A. Muharemović, H. Salkić, "Exposure to Low Frequency Magnetic Fields of a Transformer Station", International Journal of Electrical Systems Science and Engineering 1;2, 2008.

[8] B. Ćućić, "Magnetsko polje u okolini distribucijskih transformatora (Magnetic field in the vicinity of distribution transformers)", doktorska disertacija (PhD Thesis in Croatian), FER, Zagreb, 2009.

[9] B. Ćućić, Z. Haznadar, Ž. Štih, "The 3D magnetic field calculation of a dry type transformer by integral equations", The 25th International Review of Progress in Applied Computational Electromagnetics (ACES 2009), Monterey, California, 2009.